CrossMark

Aligned multi-walled carbon nanotubes (MWCNT) and vapor grown carbon fibers (VGCF) reinforced epoxy adhesive for thermal conductivity applications

Amit Kumar Singh[1,2] · Ashutos Parhi[1] · Bishnu Prasad Panda[1] · Smita Mohanty[1,2] · Sanjay Kumar Nayak[1,2] · Manoj Kumar Gupta[3]

Abstract Present study deals with the development of aligned multi-walled carbon nanotubes (MWCNT) and vapour grown carbon fibers (VGCF) reinforced epoxy adhesive system used as an alternative to Pb/Sn soldering element. The alignment of MWCNTs was carried out in a specific designed instrument exerting of an external electric field. Solution casting technique was used for the fabrication of epoxy adhesive system incorporated with aligned MWCNT and VGCF. Scanning electron microscopy and Atomic force microscopy was carried out to determine the degree of alignment of MWCNTs. Owing to the formation of continuous path for the flow of electrons, 3 wt% of aligned MWCNT with 3 wt% of VGCF reinforced epoxy adhesive achieved about five orders of magnitude higher in the thermal conductivity compared to pure epoxy. Further, the experimental results showed that the shear strength of epoxy/3% MWCNT/3% VGCF adhesive system was 112% higher than the strength of pure polymer, emphasizing the advantages of aligned MWCNT on stiffness and strength. Dynamic Mechanical Analysis and Thermo-gravimetric analysis was carried out to study the thermo-mechanical and thermal degradation behaviour of epoxy adhesive formulations.

✉ Amit Kumar Singh
singh.amit14@hotmail.com

1 Laboratory for Advanced Research in Polymeric Materials (LARPM), Central Institute of Plastics Engineering & Technology (CIPET), B-25, CNI Complex, Patia, Bhubaneswar, Odisha 751024, India

2 Central Institute of Plastics Engineering & Technology (CIPET), Chennai, Tamil Nadu, India

3 Institute for Plasma Research, Gandhinagar, Gujarat, India

1 Introduction

Polymer conductive adhesives (PCAs) open up new formulation options, which in turn lead to improved multifunctional properties as compared to other conventional polymer composites, at low fillers loading [1, 2]. In particular, carbon nanotube (CNT) based PCA offers a range of opportunities because of their unique property profile such as relatively low density and high surface area in combination with good mechanical properties and processability [3]. Accordingly, CNT based conductive adhesives are widely used for high density interconnection between sensing element [4] and cable connectors to replace the conventional lead soldering [5]. Recently in an investigation, it has been found that in liquid crystal display (LCD) applications, CNT based conductive adhesives are considered as one of the promising materials for electrical interconnection [6].

CNT based conductive adhesives have become a promising candidate for heat dissipation applications as the reinforcement phase strongly enhances their thermal diffusivity and thermal conductivity, when formation of a continuous or percolated network of interconnected nanotubes inside a polymer is achieved. CNT hybrid nanostructures showed significantly enhanced properties in a range of devices such as, thermally conductive polymeric 3D photonic crystals, broad band nano-photodetectors [7] and CNT-based chemiresistors and chemically sensitive field-effect transistors for medical applications [8]. Most of these application uses percolation network of interconnected nanotubes inside a polymer matrix for superior performance in charge separation and transfer to achieve better performance characteristics [9].

Research conducted over the past few years has shown that the mechanical properties and thermal conductivity (T_c) of the polymer composites were strongly improved by the incorporation of aligned CNT over their isotropic

⚫ Springer

counterparts. Moreover, significantly low filler content have been used to design the desired properties in the polymer matrix. Alignment of CNTs can only be accomplished by the use of external force fields such as electric, magnetic, or mechanical. Recently, the effect of alignment on the processing-structure-property relationships have been studied using electrically aligned CNT filled epoxy adhesives. Indeed, aligned CNTs have been found to produce more significant improvement in conductivity by forming point-to-point contacts between the ends of the nanotubes [10–12].

The aim of this study is to investigate the effect of the application of an electric field during the infusion of vapour grown carbon fiber (VGCF) performs using an epoxy resin reinforced with unmodified MWCNTs. VGCFs can be characterized by its high aspect ratio in the range of 250–2000, length of 100 μm, diameter of about 50–200 nm larger than CNTs with an exceptional combination of high thermal conductivity upto ~1950 W/mK [13, 14]. VGCFs can be employed in combination with MWCNTs to generate hybrid nano-adhesive system with synergistic properties. However, a cup stacked structure of VGCF comprises as additional reactive carbon terminals that can be modified to connect with the matrix resin [15].

The fabrication of electronic or microelectronic systems has recently been an emerging and highly active areas of research as it holds great promise for a number of technological applications in many fields [16]. Until now, most electronic assemblies have been typically fabricated using advantageous physical properties of aligned MWCNTs, such as excellent thermal conductivity [2], good mechanical strength [17], optional semiconducting/metallic nature [18] and advanced field-emission behaviour [19]. Therefore, there has been significant research interest recently to improve the practical applications of aligned MWCNTs that is critically important to extend their physical properties from the nanoscale to the macroscopic scale. Many research groups around the world have made multiple efforts to optimize aligned MWCNT structure and fabrication of the nanostructured materials by integrating aligned MWCNTs. In this Account, we highlighted the promising applications of aligned MWCNT composites in electronics or microelectronics assembly process. Jung et al. [20] integrated aligned CNT filled polymer hybrid architectures in diverse flexible electronic applications. The authors used aligned MWCNT filled poly dimethylsiloxane (PDMS) composites and studied its toughness against high stress conditions and reported that under such critical circumstances the composites retained its conducting nature. The authors utilized these polymer hybrid architectures directly as flexible field-emission devices. Similarly, Zhu et al. [21] developed CNT transfer technology using well aligned CNT architectures for CNT device assembly. This novel technique enabled the positioning of CNTs on temperature sensitive substrates and for the fabrication

of CNT structures for electrical interconnects, field emitters and microelectronics packaging. Another researcher, Prabakaran et al. [22] used aligned CNT filled polymer hybrid electrolytes for high performance dye sensitized solar cell applications. The authors reported that the ionic conductivity of the aligned MWCNT-electrolyte was almost double the electrolyte containing unaligned-MWCNT. Finally, Sun et al. [23] have taken aligned MWCNT architecture to one step forward with the advancement of modern electronics that need small size and light weight. In particular, aligned MWCNT architecture is an important key for the next-generation of wearable devices and biosensor networks. Moreover, there are several literatures reported on the integration of aligned CNT architecture in an electronic or microelectronic assembly process [16, 24, 25].

In this work, we present the self build alignment procedure of MWCNTs by applying an AC electric field. This technique is a very powerful enhancement technique since CNTs and wires are placed at specific locations in a more simple way to realize functional devices and circuits. Additionally, In-house fabricated alignment technique has been accepted as more cost-effective, energy efficient and environmentally benign process as compared to the traditional methods of electric field alignment. Here, MWCNTs were subjected to the passage of an AC electric field until proper alignment was achieved. Both aligned MWCNTs and VGCFs were used as fillers for the fabrication of conductive epoxy adhesive system. SEM and AFM techniques were successfully used to measure the degree of orientation of aligned MWCNTs. The thermal conductivity of different epoxy adhesive systems was measured using guarded heat flow meter method. Lap shear test was conducted in order to validate the strength of the adhesives prepared as pre-requisite for sensor interconnections. DMA and TGA analysis was also conducted to know about the viscoelastic responses and thermal degradation behaviour of epoxy adhesive systems.

1.1 Aligned CNT architectures as field effect transistors (FET)

The field effect transistor (FET) is the fundamental building block of an electronic system and its invention revolutionized the field of applied electronics, and paved the way to amplify and acts as a switch for electronic signals. The carbon-based nanostructural materials, including CNTs are highly suited for the power source of next-generation flexible and portable devices, such as, high-mobility FETs. However, the FETs based on randomly oriented CNTs usually have a poor on–off ratio that can be ambiguous for integrated circuit applications.

The process of CNT alignment described herein could hold the key to creating high density electrical interconnects used for high-mobility FETs. Additionally, the aligned

network channels of CNTs could be used as an electrode for the development of transparent flexible FETs, which also serve as a hetero-junction to provide extremely high carrier mobility, conductivity and mechanical flexibility. Aligned CNT networks are expected to show a significant improvement in the yield of CNT based FETs with a large on–off ratio while conductance changes slowly by applying a certain level of voltage [26].

Design and fabrication of electronic devices based on aligned CNT networks is similar to that reported by Lee et al. [27]. The authors have developed a technique for producing patterned self-assembled monolayer on a silicon dioxide (SiO$_2$) surface using conventional electron beam lithography. When the substrate with patterned was immersed into the CNT suspension, CNTs were selectively adsorbed onto bare SiO$_2$ surface. Figure 1 shows the schematic illustration depicting the procedure to prepare devices using aligned CNT network channels. Selective molecular assembly patterning introduced in this work suggests that through patterning the SiO$_2$ surface by alternating polar and/or non-polar self-assembled monolayer, the CNTs are able to self-assemble into desirable geometric structures. The self-assembled monolayer technique employed here takes advantage of the relative affinity between the aligned CNTs and SiO$_2$, which can be utilized to direct assembly of aligned CNTs.

The proposed methodology significantly demonstrated an improved FET performance including higher current on–off ratio and high yield fabrication of aligned CNT in FETs as reported by Lee et al. [28]. Lee et al. demonstrated improved mobility of 180 cm^2/Vs by aligning CNTs in 100 nm wide channels. It indicates that this strategy can be an ideal solution for the fabrication of the nano or micron-sized devices based on aligned CNT network channels.

2 Materials and methods

2.1 Materials

Diglycidyl ether of bisphenol-A (DGEBA, Araldite GY 250) resin with epoxy equivalent weight (E.E.W.) of 180–189 g/Eq. used as a base matrix; Triethylenetetramine (TETA, Aradur HY951) with amine value of 520–580 mg KOH/g used as a hardener, were purchased from M/s Huntsman Advanced Materials Pvt. Ltd., India. MWCNTs produced by catalytic chemical vapour deposition (CCVD) method were purchased from M/s Sigma Aldrich Pvt. Ltd., India. MWCNTs have an avg. outer diameter of 6–13 nm, avg. length of 2–20 μm and purity of >98%, as per the supplier's specification. A commercially available carbon fiber (VGCF, Pyrograf-III) with an avg. diameter of 100 nm, surface area of 43 m^2/gm and avg. purity of >92% was purchased from M/s Sigma Aldrich Pvt. Ltd., India. Common chemical such as acetone was purchased from M/s Merck Specialists Pvt. Ltd., India.

2.2 Methods

2.2.1 Fabrication of MWCNT and VGCF reinforced different epoxy adhesive systems

Based on the mixing ratio of epoxy and hardener, the following quantities were mixed during the fabrication of different epoxy adhesive system. Table 1 shows the different epoxy adhesive formulations and the mixing ratios for the investigated systems.

Prior to the fabrication of epoxy/3% MWCNT/3% VGCF adhesive system, the total mass of the resin taken was typically about 130 gm. The optimum resin-to-hardener ratio

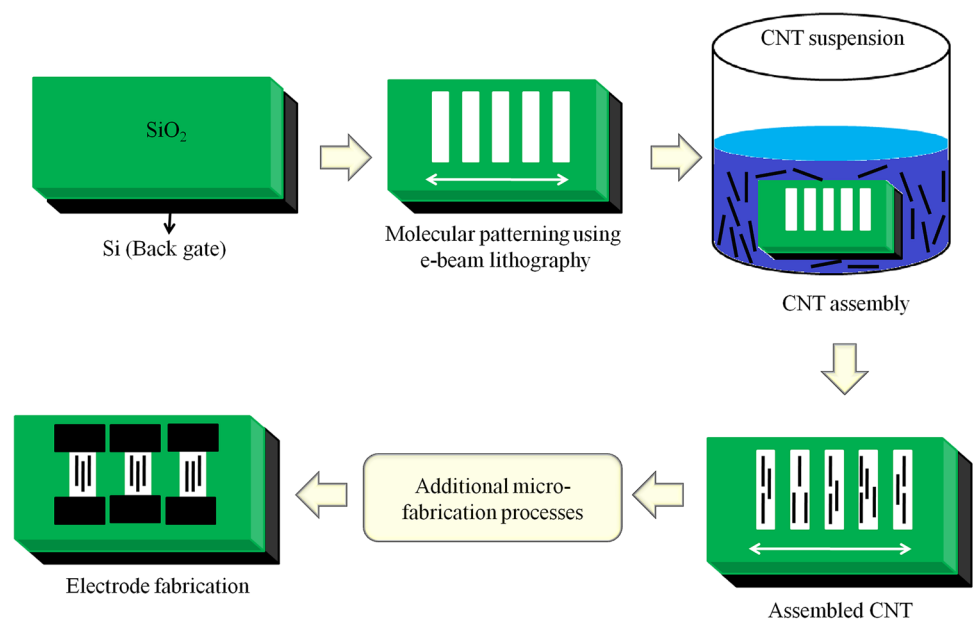**Fig. 1** Schematic diagram depicting the procedure to prepare devices using aligned CNT network channels

Table 1 Different epoxy adhesive formulations

Sample type	Quantity (gm)			
	Epoxy resin	Hardener	MWCNT	VGCF
Epoxy	130	13	–	–
Epoxy/1% VGCF	128.7	13	–	1.3
Epoxy/2% VGCF	127.4	13	–	2.6
Epoxy/3% VGCF	126.1	13	–	3.9
Epoxy/5% VGCF	123.5	13	–	6.5
Epoxy/1% MWCNT	128.7	13	1.3	–
Epoxy/2% MWCNT	127.4	13	2.6	–
Epoxy/3% MWCNT	126.1	13	3.9	–
Epoxy/5% MWCNT	123.5	13	6.5	–
Epoxy/1% MWCNT/1% VGCF	127.4	13	1.3	1.3
Epoxy/2% MWCNT/2% VGCF	124.8	13	2.6	2.6
Epoxy/3% MWCNT/3% VGCF	122.2	13	3.9	3.9
Epoxy/5% MWCNT/5% VGCF	117	13	6.5	6.5

was maintained at 100:10, to achieve maximum degree of curing. Masses of fillers were calculated based on the total mass of resin, as a result 3 wt% of MWCNT (3.9 gm) and 3 wt% of VGCF (3.9 gm) was measured. The calculated amount of MWCNTs and VGCFs were immersed in acetone using high speed mechanical stirrer, achieving homogeneous dispersion of fillers within epoxy resin. Afterwards the epoxy resin was added to the reaction mixture followed by sonication (DT-151, 3.5 L capacity M/s Darsh Technologies Ltd) for another 1 h. The reaction mixture was then kept in a vacuum oven for at least 6 h to remove the acetone completely. Finally it was cooled to room temperature, curing agent was added with gentle mixing for 5–10 min, poured into a metallic mold at 60 °C for 6 h. The other epoxy adhesive systems with different content of fillers were prepared with exactly the same procedure described above.

2.2.2 In-house fabrication of alignment setup and procedure for alignment of epoxy/MWCNT conductive adhesive system

Fabrication of an alignment device consists of a mold composed of two aluminium electrodes fixed to a glass substrate, as shown in the Fig. 2b. The experimental design approaches presented here were applied successfully for facilitating reliable parameter estimates and using the best parameter values for a particular set of data. An alignment setup has been designed and constructed for the purpose of conducting experiments under electric field.

The distance between the two aluminium electrodes was maintained at a constant distance of 5 mm and thickness was roughly in the range of 3 mm. A glass substrate was kept on the top of the mold, make sure that the top surface is as flat as possible that facilitates accurate timely requirements

monitoring, minimizes risk and supports flexibility. To produce an AC electric field, the mold was connected to a wave-front generator (M/s UNOPOS Bhubaneswar, India), which produces output power ranging from a few 100 mW up to hundreds of W using a power amplifier. Copper wire was used to make electrical interconnection between different parts of the assembly process. Copper also provides superior thermal conductivity which saves energy and accelerates the heat dissipation process. This property is especially helpful at connections and terminations of the alignment assembly. The alignment setup also consists of a power switch for on–off purpose of the output voltage amplifier.

Before exertion of an AC electric field, a release agent (i.e. silicon) was sprayed on the mold. Then, the prepared epoxy adhesive sample was poured within the mold, make sure that no air bubbles were formed within the mold. After few moments, electric field at a constant output voltage of 240 V, at a frequency of 50 Hz was applied to epoxy adhesive sample. The wave front generator was turned on to produce an AC electric field. At this time, the temperature of the whole alignment setup was maintained at 60 °C. After 6 h of maintaining temperature and AC supply, the wave front generator was shut down properly only when epoxy adhesive was cured completely. Figure 2a shows instrumentation for the in-house fabricated electric field alignment setup and Fig. 3 depicts the schematic illustration for the method of preparation of aligned MWCNT and VGCF filled epoxy adhesive system.

3 Characterization techniques

3.1 Scanning electron microscopy (SEM)

The degree of alignment of MWCNTs and interaction of fillers within polymer matrix was investigated using a scanning
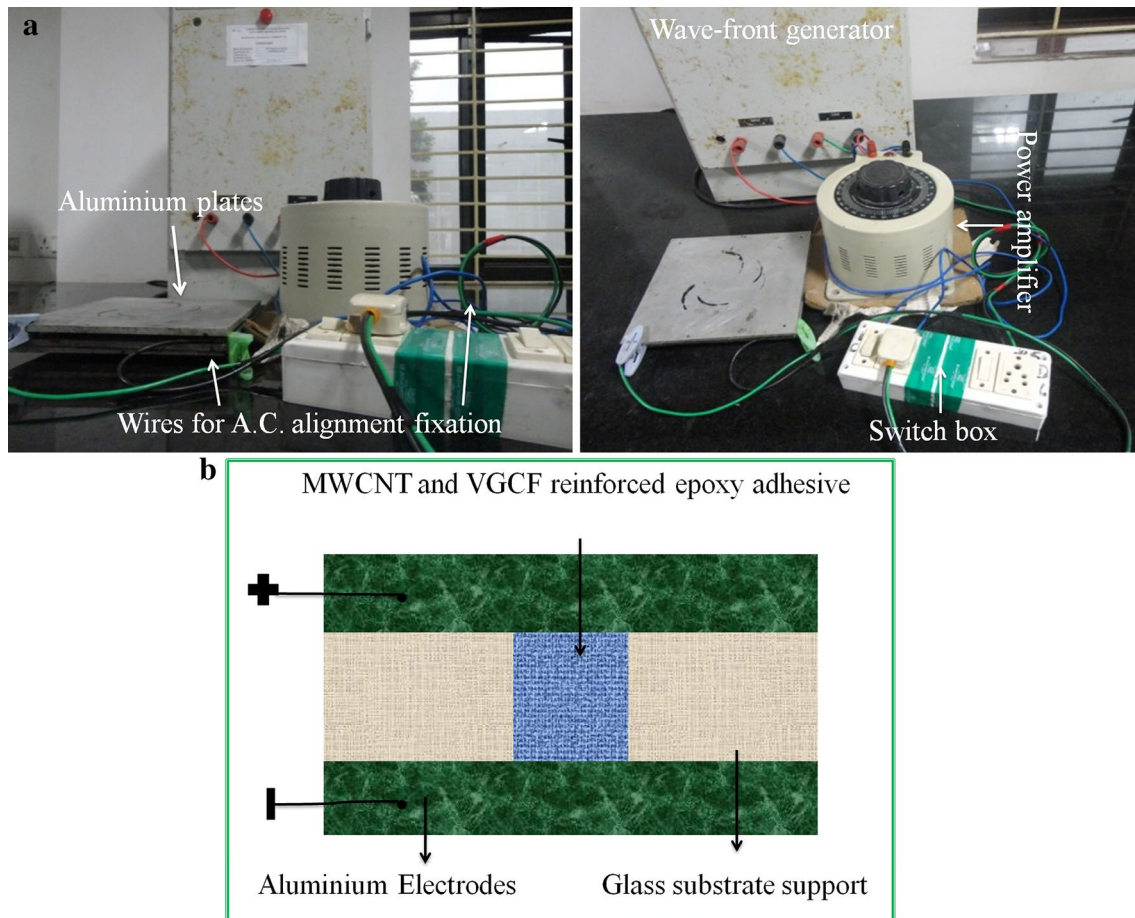
Fig. 2 Assembly of in-house fabricated electric field alignment setup (**a**) and schematic of a mould used for electric field alignment of MWC-NTs (**b**)

electron microscope, EVO MA 15 (Carl Zeiss SMT, Germany). Prior to analysis, the samples were sputter coated with Au/Pd mixture to avoid electric discharge. All the samples were tested at an accelerating voltage of 5 kV and micrographs were taken at scale bars of 10 μm.

3.2 Atomic force microscopy (AFM)

AFM images of different epoxy adhesive systems were taken using atomic force microscope, Park XE-100 Japan Inc., working in non-contact mode. The 3-D topographic images were taken with a resolution of 512×512 pixel and at a scanning frequency of 0.5 Hz.

3.3 Lap shear test

The mechanical properties of epoxy adhesive systems reinforced with different wt% of fillers were measured using Universal Testing Machine (UTM, 3382 Instron, UK) and tested in accordance with ASTM D 1002 standard. Aluminium was used as a substrate with an adhesive lap area of 12.7 mm, test grip area of 25.4 mm and at a crosshead speed of 1.27 mm/min.

3.4 Thermal conductivity measurement

The thermal conductivity of all epoxy adhesive samples was measured using Unitherm 2022 M/s Anter Corporation, USA based on the ASTM E 1530 guarded heat flow meter method. All the samples were tested at 30 °C and the dimensions of the round shape test samples were 50 mm diameter by 3 mm thick.

3.5 Thermo-gravimetric analysis (TGA)

Thermal decomposition temperature of epoxy adhesive samples was obtained using thermo-gravimetric analyzer TGA Q 50 M/s TA instruments, USA, under an inert atmosphere.
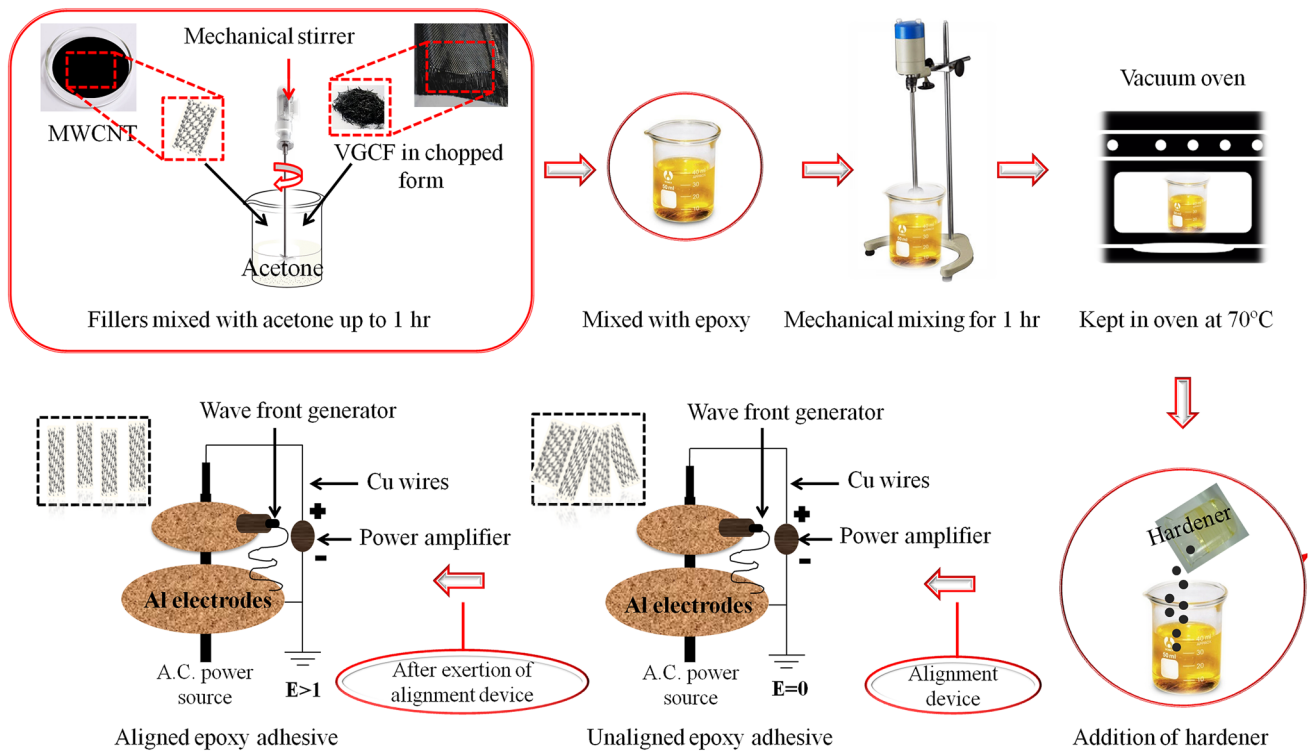
Fig. 3 Schematic illustration for the method of preparation of aligned MWCNT and VGCF filled epoxy adhesive system

Usually, 5–10 mg of sample was heated from 30 to 700 °C, at heating rate of 10 °C/min according to the ASTM E 1641-04 standard.

3.6 Dynamic mechanical analysis (DMA)

The visco-elastic responses of cured epoxy adhesive samples were determined using dynamic mechanical analyzer DMA Q 800 M/s TA instruments, USA. Test was performed for all samples of dimension $63.5 \times 12.7 \times 3.2$ mm, at a frequency of 1 Hz. Epoxy adhesive samples were heated from 30 to 150 °C, at a heating rate of 10 ºC/min with the three point bending mode as per the ASTM D 5026 standard.

4 Results and discussion

4.1 Confirmation of degree of alignment of MWCNTs

4.1.1 Scanning electron microscopy (SEM) analysis of epoxy adhesive system

The matter is completely unarguable since there is no direct experimental evidence available for the confirmation of degree of alignment of MWCNTs. Therefore, it is our goal to evaluate the physical and morphological characteristics of aligned MWCNTs from SEM microscopy [29–31].

SEM micrographs as obtained for epoxy, epoxy incorporated with aligned MWCNTs and epoxy incorporated with hybrid fillers, MWCNT and VGCF are shown in the Fig. 4a–f, respectively. SEM micrograph of epoxy adhesive shown in Fig. 4a predicted rather smooth and homogeneously dispersed surface. Figure 4b for epoxy adhesive incorporated with 3 wt% of aligned MWCNTs resulted in the formation of regular protrudes evenly distributed over the whole surface of the epoxy adhesive system [32]. These protrudes came into sight in the form of the bright lines. These bright lines indicating production of controlled lamellar architectures of aligned MWCNTs.

Whereas SEM micrographs for the epoxy incorporated with 3 wt% of aligned MWCNT and 3 wt% of VGCF at different magnifications (scale bar of 10 μm for all micrographs) are shown in Fig. 4c–f. Figure 4c shows formation of homogenous protrudes arising from the fine embedding of aligned MWCNTs without any de-bonding or pull-out of MWCNTs. Hence, the electrically charged MWCNT network was stretched across the matrix to provide thermal conductive pathways throughout the adhesive system and finally resulted in higher T_c of the cured epoxy adhesive system. The reinforced epoxy adhesive systems are highly cross-linked network structure but epoxy resin has serious drawback in terms of their brittleness with a poor resistance to crack [33], which limit its applications. However, incorporation of a second phase of dispersed VGCF within
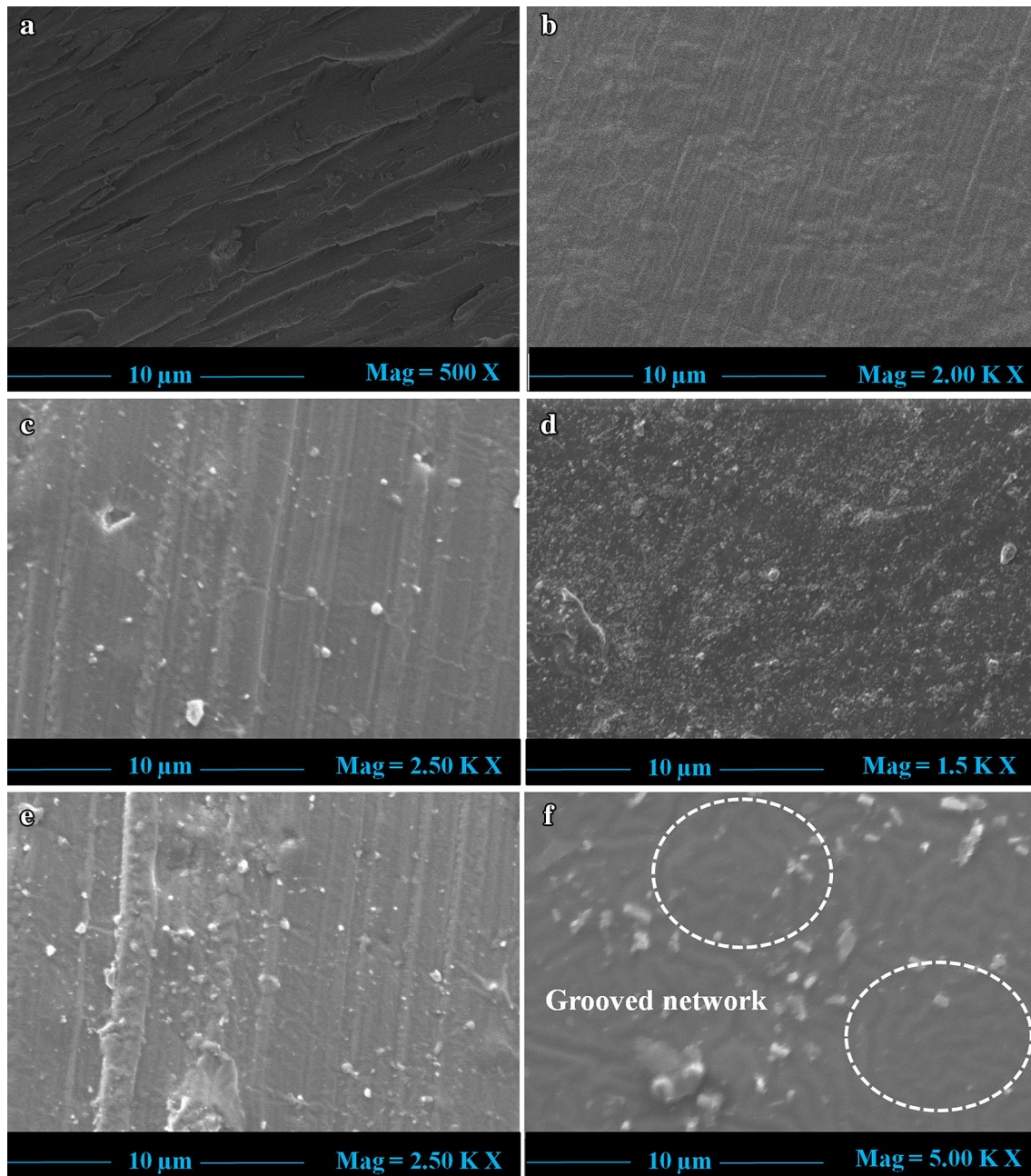
Fig. 4 SEM micrographs of epoxy only (**a**), epoxy/3 wt% MWCNT adhesive at 2.00 KX (**b**) and epoxy/3 wt% MWCNT/3 wt% VGCF adhesive at 2. 50 KX (**c**), at 1510 X (**d**), at 2.50 KX (**e**) and at 5.0 KX (**f**) magnification scale

epoxy can greatly increase their toughness, while maintaining lamellar structure of aligned MWCNTs.

The SEM micrograph for the epoxy/3% MWCNT/3% VGCF adhesive shown in Fig. 4d is well aligned and fully extended. However, the surface of adhesive was found to be rough and irregular due to aggregation of the VGCF during the alignment procedure. Figure 4e shows the SEM micrographs of the adhesive prepared parallel to the alignment direction. The presence of lamellar structures

of aligned MWCNTs in the epoxy is indicative of the existence of crystalline regions [34]. From Fig. 4f presence of grooved network can also be observed, which further strengthened the presence of aligned filler network in epoxy. The reason behind the presence of a grooved network is, since epoxy being a thermoset material with high yield strength therefore, there was no possibility of shrinkage and warpage on curing and only one possibility left behind which is the formation of an aligned network of

nano-fillers within the epoxy. Since, MWCNT and VGCF have high intrinsic thermal conductivity [35–37] therefore, using aligned MWCNT and VGCF incorporated within epoxy resulting in decreasing the contact area between conductive fillers and epoxy. As a result, lesser phonon scattering at the matrix-filler interface and therefore resulted in an effective phonon transfer at the boundary.

4.1.2 Atomic force microscopy (AFM) analysis of epoxy adhesive system

One-dimensional fillers such as CNT having large aspect ratio and high surface area plays an important role in increasing the thermal transport properties of CNT reinforced conductive adhesives. Since CNTs considered as an anisotropic, therefore realizing the full potential of CNTs they should be aligned in one particular direction.

AFM images as obtained for the epoxy conductive adhesive system are used in understanding the degree of orientation i.e. either parallel or perpendicular to the field direction inside the viscous polymer matrix. The AFM images for epoxy incorporated with aligned MWCNTs are shown in Fig. 5a, b. From Fig. 5a, it is observed that MWCNTs were aligned along the applied electric field direction due to direct MWCNT–MWCNT interactions. It is also noticed that area near the wire grids had lighter in colour than mid-gap areas, suggesting less MWCNTs were existed near wire grids [38]. It is also clear from the topographical image as shown in Fig. 5b for epoxy incorporated with 3 wt% of aligned MWCNT that, MWCNT density resulting in absolute definiteness of MWCNT orientation, which confirmed the crowding effect as the alignment for MWCNTs [39]. Figure 5b indicated that the alignment process increases the roughness of the adhesive system to ~500 nm or less. AFM micrographs also confirmed good dispersion of aligned MWCNTs within epoxy with no sign of aggregation, which is the preliminary requisite for the formation of aligned filler network. The aligned fillers forming a pathway across the epoxy matrix and thus can be fruitful in transferring the heat energy across the adhesive thickness.

Figure 5c, d shows AFM images of the epoxy incorporated with 3 wt% of aligned MWCNT and 3 wt% of VGCF.
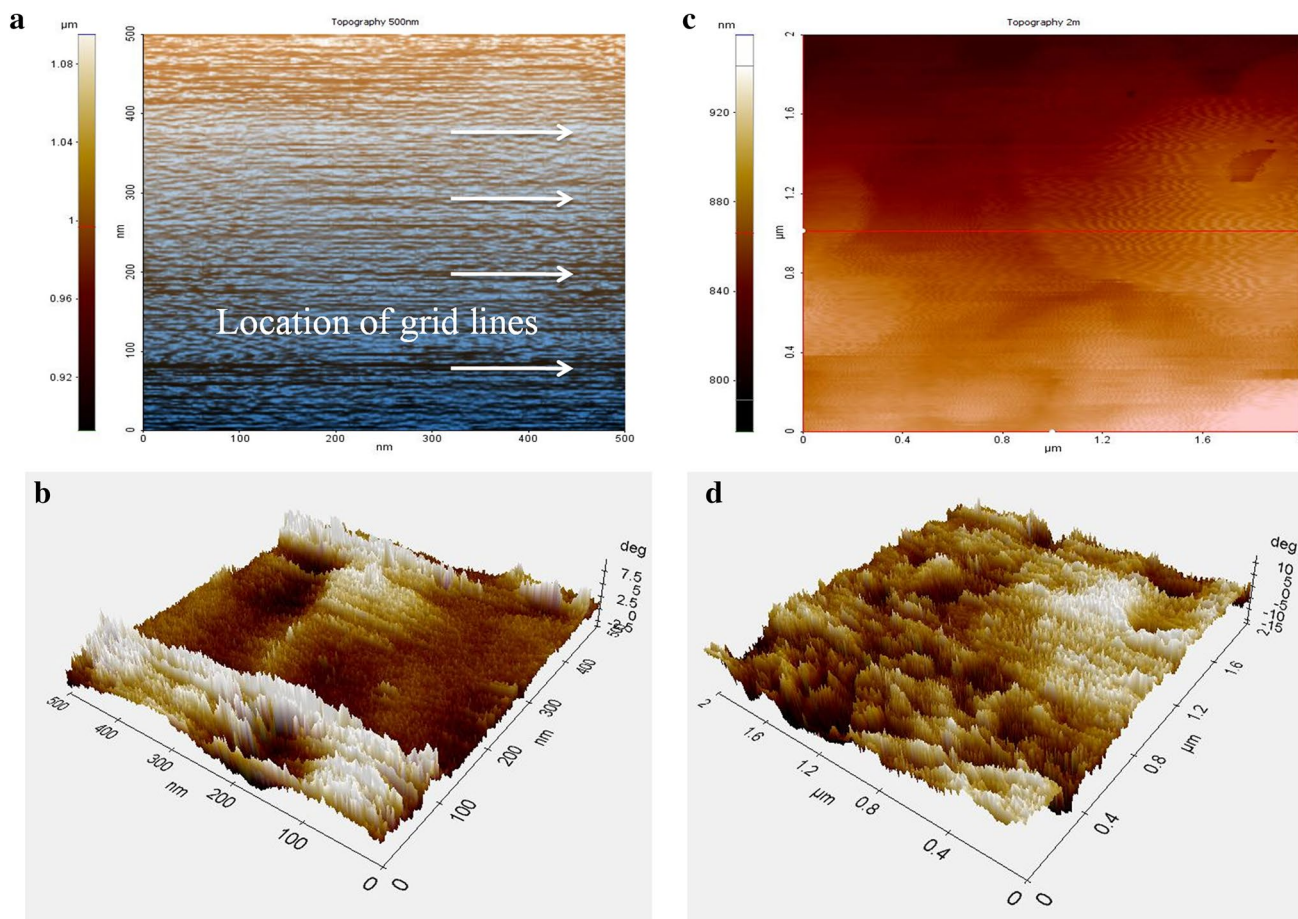
Fig. 5 AFM micrographs for epoxy/3 wt% MWCNT (**a, b**) and epoxy/3 wt% MWCNT/3 wt% VGCF (**c, d**) adhesive system

Figure 5c shows large smooth areas corresponding to the aligned MWCNTs and small entities identifiable as VGCF, forming a dark phase. Brighter areas in the Fig. 5c may be attributed to the greater force experienced by aligned MWCNT during scanning whereas the darker areas visible in the image correspond to amorphous phase due to interaction between epoxy matrix and VGCF [40].

4.2 Thermal conductivity (T_c) measurement of epoxy adhesive system

The thermal conductivity (T_c) measurements made in this study for epoxy adhesive systems were performed at room temperature. The T_c values for epoxy, epoxy/aligned MWCNT, epoxy/VGCF, epoxy/aligned MWCNT/VGCF and epoxy/unaligned MWCNT adhesive systems are summarized in Table 2.

The T_c of different epoxy adhesive system increases sharply over the range from 1 to 3 wt% of filler loading, indicating a percolation threshold at 3 wt%. At the percolation threshold, the T_c increases about 85, 225 and 370% for epoxy/VGCF, epoxy/MWCNT and epoxy/MWCNT/VGCF adhesive system respectively, as compared to pure epoxy. The epoxy incorporated with 3 wt% of aligned MWCNT have T_c about 0.65 W/mK which is 75.6% increase over epoxy/VGCF adhesive system at 3 wt% of VGCF loading. This is probably due to the fact that VGCF within the epoxy matrix are not connected with each other and does not form sufficient thermal conductive pathways as confirmed from the SEM micrograph shown in Fig. 6.

SEM micrograph of fracture surfaces of epoxy/3% VGCF adhesive system as shown in Fig. 6 revealed a non-uniform dispersion of the VGCFs within the polymer matrix. In addition to this, other notable features included a few aggregates and a portion of VGCFs are pulled out from the polymer matrix leaving voids at the filler and polymer interface. These observations reveal the weak interfacial adhesion between VGCF and epoxy and become less convenient from the perspective of formation of interconnected networks. Alternatively, an observation of the SEM micrograph shown in Fig. 7a indicated that

increasing the content of VGCFs to 5 wt% yield surfaces with higher coarse aggregate contents. A larger aggregate may cause more surface voids and the most likely reason of a low T_c as compared to 3 wt% of filler content.

The effective T_c enhancement for the epoxy incorporated with aligned MWCNT depends on many physical properties such as MWCNT density, contact resistance, surface properties and mainly on the inherent thermal conductivity of MWCNTs. MWCNTs are attached to each other by strong Van-der Waals forces, which is pre-requisite for heat transport in aligned MWCNTs. When aligned MWCNTs overlap with each other, heat first flows through an outermost shell of one nanotube and then penetrate into innermost shells of second nanotubes. As soon as the heat is introduced, the two dimensional graphene layer of nanotubes have a significant effect on heat transport and indicated an important effect of reverse/re-circulation flow, which promotes the heat transfer in aligned MWCNTs [41]. This resulted in an increased T_c for epoxy/MWCNT adhesive system, at 3 wt% of filler loading.

However, a decrease in the T_c of epoxy/aligned MWCNT adhesive is noticed with increasing the wt% of filler loading, above the percolation threshold, that is, at 5 wt% of aligned
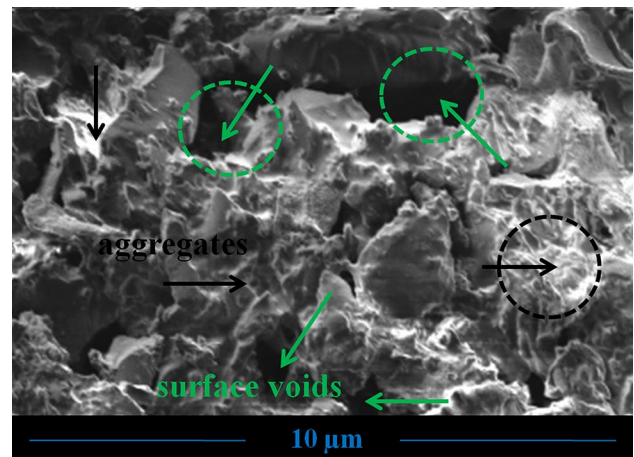

Fig. 6 SEM micrograph for epoxy/VGCF adhesive at 3 wt% of filler loading

Table 2 Thermal conductivity values for different epoxy adhesive system

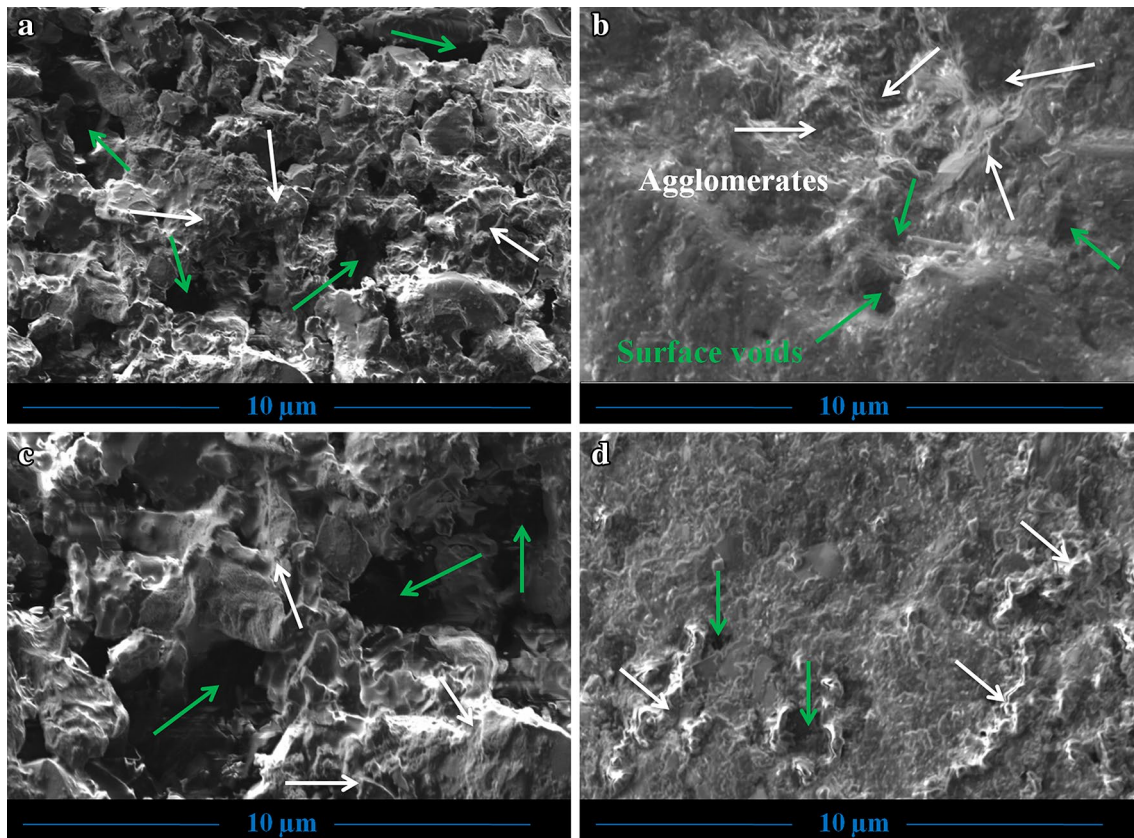| Filler content (wt%)	Thermal conductivity (T_c, W/mK)				
	Epoxy	Epoxy/VGCF	Epoxy/aligned MWCNT	Epoxy/aligned MWCNT/VGCF	Epoxy/ unaligned MWCNT
0	0.20	–	–	–	–
1	–	0.26	0.54	0.84	0.29
2	–	0.31	0.59	0.89	0.36
3	–	0.37	0.65	0.94	0.49
5	–	0.36	0.61	0.87	0.45

Fig. 7 SEM micrographs for epoxy/VGCF (**a**), epoxy/aligned MWCNT (**b**), epoxy/MWCNT/VGCF (**c**) and epoxy/unaligned MWCNT (**d**) at 5 wt% of fillers loading

MWCNT. This decrease may be attributed to the fact that the 3D thermal conductive pathways were not formed due to the presence of surface voids and agglomerates in epoxy adhesive system (as shown in Fig. 7b) and thus the conductivity is only due to the tunneling conduction mechanism or direct contact between the aligned MWCNTs [42].

As expected, epoxy incorporated with 3 wt% of aligned MWCNT and 3 wt% of VGCF provides the highest value of T_c and reached upto 0.94 W/mK. Similar results have been reported by Gonnet [43] and Fisher et al. [44] VGCF is an ideal thermally conductive filler due to its high inherent T_c of ~1950 W/mK [42]. As a result, VGCF along with aligned MWCNTs, making a net tunneling effect by forming an aligned network of the fillers within epoxy. This enabled the phonons to pass along the thickness of the adhesive and improving its T_c [45, 46]. This increase may be attributed to the formation of well organized heat circulating path in aligned MWCNTs passes through VGCF because of acoustic phonons and uniform dispersion of aligned MWCNT and VGCF within epoxy [47]. However, at 5 wt% of filler loading, decrease in T_c was noticed for 3 wt% of aligned MWCNT with 3 wt% of VGCF filled epoxy adhesive. Above the percolation threshold, a decrease of about 8% was

observed as compared to epoxy adhesive incorporated with 3 wt% of aligned MWCNT and VGCF loading. As evident from the SEM micrograph shown in Fig. 7c, the decrease in T_c may be attributed to the poor homogeneity of the fillers surface, presence of agglomeration and availability of surface voids, depending on the dimension and degree of distribution of aligned MWCNT and VGCF.

However, some of the MWCNTs are in fact oriented in the transverse or Y-direction. The T_c in the Y-direction for the epoxy adhesives incorporated with aligned MWCNT and combination of aligned MWCNT and VGCF were also measured and compared with T_c in axial or X-direction. Figure 8 shows the results of comparison of T_c for epoxy/aligned MWCNT and epoxy/aligned MWCNT/VGCF in X- and Y-directions. The T_c values in the Y-direction for epoxy/aligned MWCNT and epoxy/aligned MWCNT/VGCF adhesive systems are 0.25 and 0.91 W/mK, respectively, at 3 wt% of fillers loading. The nonlinearity of the T_c in Y-direction for the epoxy/aligned MWCNT adhesive remains near the T_c of epoxy resin. It can also be concluded that the T_c in the X- and Y-directions are roughly equal in case of two dimensional epoxy/aligned MWCNT/VGCF adhesive system.

Similar observations were also observed by Chen et al. [48] in the case of aligned VGCF reinforced epoxy composites.

Thermal conductivity as a function of filler content for epoxy adhesive incorporated with unaligned MWCNTs was also measured and values have been summarized in Table 2, for comparison purpose. Also, for epoxy/unaligned MWCNT an increasing trend in T_c was observed with an increase in filler content. In particular at 3 wt% of unaligned MWCNT loading, an increase of about 125% was observed as compared to the pure epoxy. However, T_c of epoxy/ unaligned MWCNT is low as compared to epoxy/aligned MWCNT, at each filler loading. At percolation threshold, a decrease of about 32.6% was observed for epoxy/unaligned MWCNT as compared to epoxy/aligned MWCNT adhesive. It may be attributed that aligned MWCNTs are expected to exhibit enhance T_c due to the reduced number of interface and contact resistance. Additionally, the phonon transports were found to be preferably oriented in the aligned direction of MWCNTs in the adhesives. It also associated with a number of phonon vibrational modes and higher mean free path in the crystalline graphite structures as compared to unaligned MWCNTs [49]. However, the T_c was noticed a decrease upto 8.8% with an increase in the MWCNT content upto 5 wt%. Once more the result suggest the presence of MWCNT aggregates that can lead to the formation of surface voids, which is substantiated in our experimental findings as shown in Fig. 7d.

Similar observations were reported by Ghose et al. [50] where a significant enhancement in T_c up to 24-fold was observed when T_c measurements were made parallel to the tube axis. The authors proposed a composite configuration where embedded CNTs are aligned from one surface to the opposite side, forming a network to successfully conduct heat, by perhaps enabling a more efficient phonon transfer from one filler particle to another. Low interfacial thermal resistance can also be expected in case of aligned CNT composites, since the protruding tips would ensure better thermal contact. Huang et al. [51] also observed the same trend in case of aligned CNT composite films. These findings provided further evidence that the prominent thermal properties of aligned CNTs are often regarded as one of the most promising candidates for future applications in thermal management for e.g. nano-electronics.

4.2.1 Working principle of aligned MWCNT and MWCNT/ VGCF filler system

In order to enhance the T_c of epoxy resin, thermally conductive materials should be introduced to form composite materials. MWCNTs have long been used as fillers for epoxy resin composites in scientific community. The fact has been substantiated by many investigators such as Liao et al. [52] that the aligned MWCNT composites have higher T_c than unaligned MWCNT composites. The analyses indicate that the composite not only take advantage of the high T_c of MWCNTs, but also enhances the thermal conduction of epoxy chains.

When aligned MWCNTs are introduced into composites, the T_c in the axial direction of aligned MWCNTs is much higher than randomly oriented MWCNTs. The high performance of aligned MWCNT in polymer matrix is often attributed to the low interfacial thermal resistance in addition to low tube–tube contact resistance [53]. Besides interfacial thermal resistance, filler–filler contact resistance, dispersion of fillers and percolation threshold, the contact (overlapping) area of fillers should also be a very important factor for heat conduction within the polymer matrix. The formation of conductive network among fillers within the polymer matrix can be significantly achieved only when the conductive particles are in close proximity to each other. It may be attributed to the fact that the ratio of thermal conductivities between filler and matrix is much smaller than that of
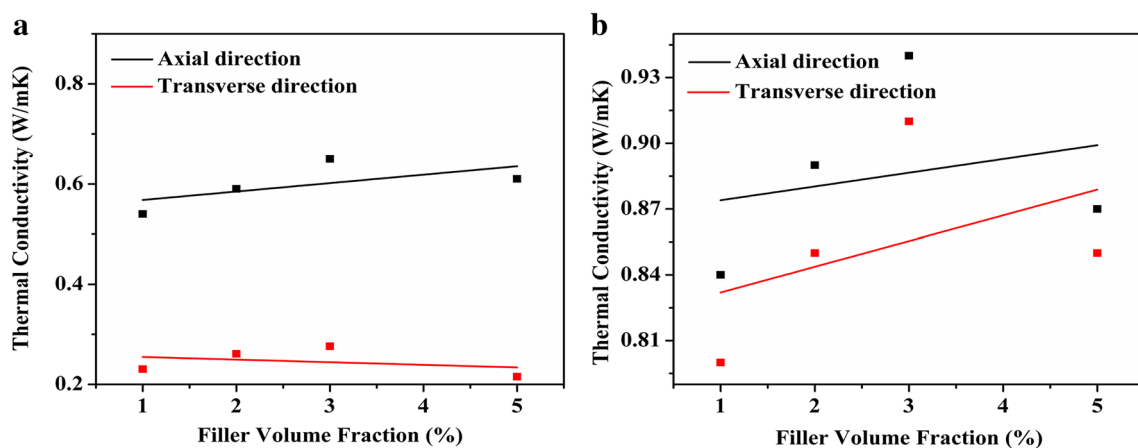

Fig. 8 Comparisons of thermal conductivity for epoxy/aligned MWCNT and epoxy/aligned MWCNT/VGCF adhesives in X- and Y-direction

electron conductivities [54]. The three dimensional composite structures and heat transfer directions in case of epoxy/aligned MWCNT and epoxy/aligned MWCNT/VGCF is illustrated in Fig. 9. The degree of overlap on the interfacial area is strongly influenced by the morphology of conductive particles and it increases as the filler particle deviates from perfect surface morphology i.e. aspect ratio. While showed in Fig. 9, the significant increase in T_c of epoxy composites is associated with the interaction between one-dimensional aligned CNTs and matrix resin. The interactions between aligned nanotubes and matrix resin are considered to be point-to-point. Accordingly, thermal conductive pathways are preferentially produced along the alignment direction due to the reduced interface and thermal contact resistance. Similar observations were observed by Gonnet et al. [41] in the case of aligned CNT buckypapers and composites.

Whereas in the case of epoxy/aligned MWCNT/VGCF adhesive system, the interaction between aligned MWCNTs, two-dimensional VGCF fillers and matrix resin is considered to be face-to-face. It is also evident that, two-dimensional fillers can provide much larger area of overlap, which might make them promising thermal conductive fillers and one of the reasons for such high T_c obtained in this work. Similar observation was also noticed by Lin et al. [55] Additionally, the two-dimensional structure of VGCF creates a significant contact area with the aligned MWCNTs because both the top and bottom surfaces of aligned MWCNTs are in close contact with the VGCF, serving as heat conducting bridges

between aligned MWCNTs and matrix resin. Therefore, formation of an efficient 3D network for heat transport within a polymer matrix is pre-requisite for enhanced T_c, which has been substantiated in our experimental findings.

4.3 Lap shear test

In this section, mechanical properties of different epoxy adhesive system were evaluated. A new lap-shear test geometry which reduces the difficulties associated with specimen preparation is introduced, and complex stress–strain behavior is taken into account. By varying the filler content from 1 to 5 wt%, a variation in the shear strength was observed and important findings have been summarized in Table 3. Figure 10 shows the corresponding stress–strain curve for different epoxy adhesive system.

From Table 3, it is clear that the shear strength of epoxy adhesive system increased consistently with increasing the wt% of MWCNTs (from 1 to 3 wt%). The addition of 1 wt% of MWCNT into unmodified epoxy has resulted in significant improvement in the shear strength up to 4.5 MPa. Moreover, with the addition of 3 wt% of MWCNT, the shear strength of epoxy adhesive increases up to 5.9 MPa, that is, approximately a 47.5% increase in strength is observed as compared to pure epoxy. Which is due to the high specific surface area and reinforcement effect of the MWCNTs within the polymer matrix [56]. Additionally, homogeneous dispersion of MWCNTs in polymer matrices play a key role
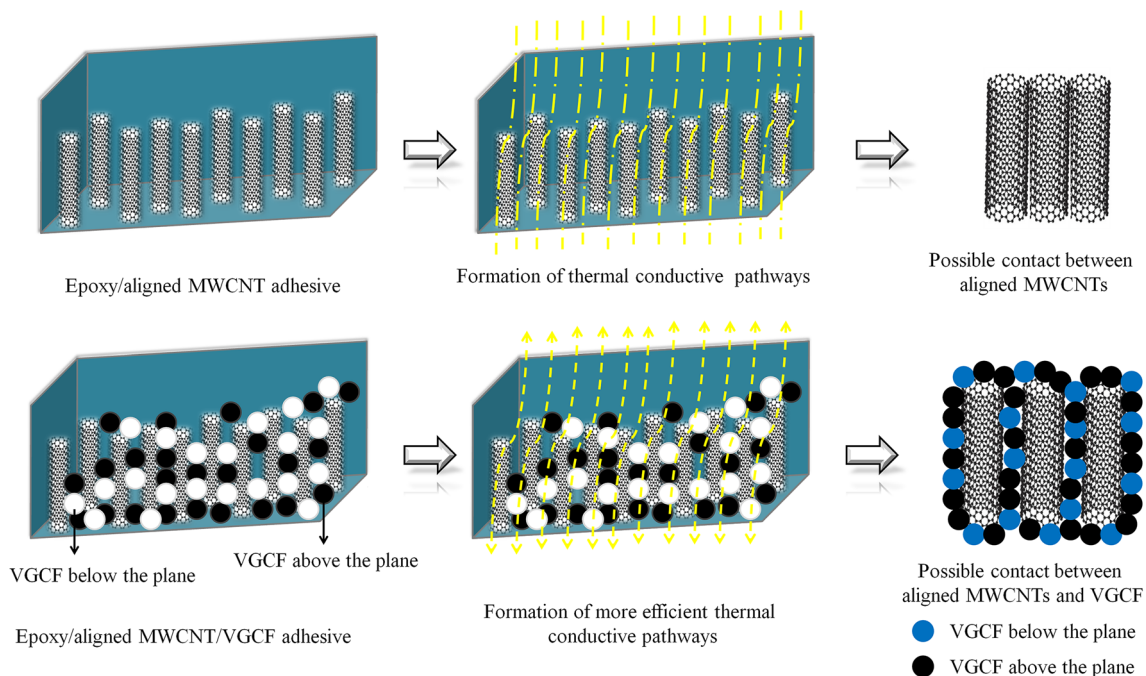

Fig. 9 Formation of thermal conductive pathways for epoxy/aligned MWCNT and epoxy/aligned MWCNT/VGCF adhesive system, the *arrows* indicate the direction of heat flow

Table 3 Mechanical properties for different epoxy adhesive system

| Sample type	Shear strength (MPa)	Shear modulus (MPa)	Elongation at break (%)	Type of failure
Epoxy	4.0 ± 1.2	2950 ± 40	0.23 ± 0.01	Adhesive
Epoxy/1% MWCNT	4.5 ± 1.8	2975 ± 45	0.22 ± 0.05	Partly cohesive
Epoxy/2% MWCNT	4.7 ± 3.1	2460 ± 32	0.3 ± 0.01	Partly cohesive
Epoxy/3% MWCNT	5.9 ± 2.3	2290 ± 35	0.55 ± 0.04	Fully cohesive
Epoxy/5% MWCNT	5.0 ± 1.9	2340 ± 29	0.35 ± 0.02	Cohesive
Epoxy/3% MWCNT/3% VGCF	8.5 ± 2.0	2420 ± 37	0.63 ± 0.03	Fully cohesive
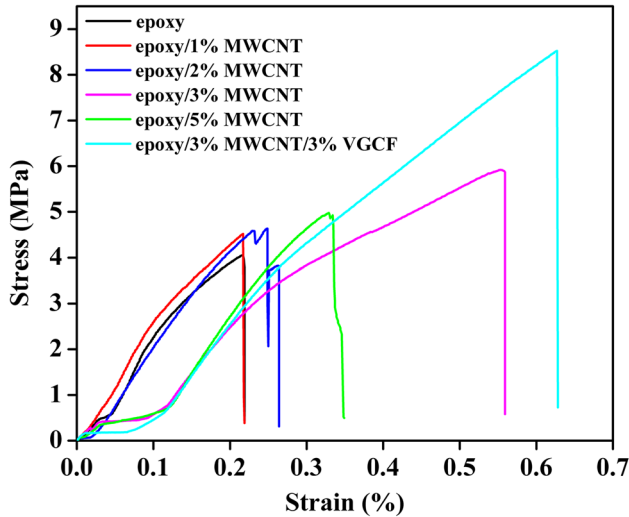
Fig. 10 Stress vs strain curve for different epoxy adhesive system

in determining the properties of epoxy adhesives [57]. At 3 wt% of filler content, MWCNTs are dispersed uniformly through the polymer matrix, which facilitates the formation of good interfacial adhesion between MWCNTs and polymer matrix. Good interfacial adhesion enables stress to be effectively transferred from the polymer matrix to the fillers [58, 59]. As a result, epoxy/MWCNT adhesive provides higher shear strength, at 3 wt% of MWCNT loading.

The shear strength of epoxy adhesives incorporated with 3 wt% of MWCNT and 3 wt% of VGCF was also measured and compared with strength of epoxy/MWCNT adhesive, at 3 wt% of filler loading. With an addition of 3 wt% of VGCF within epoxy/MWCNT framework, higher shear strength value was observed. Using VGCF improves interaction between the MWCNTs and polymer matrix and hence dispersion. The effective dispersion of fillers in a polymer matrix allows stress to be effectively transferred from the polymer matrix to MWCNTs and then to stiffer VGCF fibers. Moreover, uniform dispersion of MWCNTs in the polymer matrix acts as a bridge between epoxy and VGCFs, which leads to the development of mechanical interlocking mechanism. This mechanism in turn, increases the load-bearing

ability of the whole adhesive system during tensile loading. When epoxy/3% MWCNT/3% VGCF adhesive was subjected to tensile loading under maximum load, crack initiates and propagates within the matrix first, as being the lowest modulus component in the three phase adhesive system. A load is then transferred from the matrix to fibers through mechanical interlocking mechanism. Thus, energy-absorbing ability of the entire adhesive system increases, which increases the strength of whole epoxy adhesive system [60]. Similar findings were also observed by Shen et al. in the case of improvement of mechanical properties of natural fiber composites via carbon nanotube addition [61].

However, the shear strength of epoxy adhesive incorporated with 5 wt% of MWCNT has reduced by 18% when compared with epoxy/MWCNT, at 3 wt% of MWCNT loading. A decrease in strength is mainly attributed to the agglomeration of MWCNTs and stress concentration at the agglomeration areas which initiates the crack propagation in adhesive joints.

Meanwhile, a decrease of shear modulus is also observed for epoxy/MWCNT, at different reinforcement content of fillers. The pure epoxy showed a shear modulus value of 2950 MPa. The addition of 2 wt% MWCNT decreased the shear modulus of the pure epoxy by 20%. Whereas, the shear modulus decreased from 20% for the epoxy/2% MWCNT to 28.8% for the epoxy adhesive incorporated with 3 wt% of MWCNT loading. Decrease in shear modulus may be attributed to the attractive forces between the graphite nano-platelets of MWCNTs that leads to agglomeration of MWC-NTs in the polymer matrix. However, the tensile modulus of epoxy/3% MWCNT adhesive increased with adding 3 wt% of VGCF loading due to the reinforcement effect of fibers. Increase in shear modulus for epoxy/3% MWCNT/3% MWCNT may be attributed to the proper adhesion between three component adhesives with one part being VGCF. The stiffer the adhesive system under shear stress, the more efficiently the load transfer between fibers. Therefore, stress concentration in the neighbouring fibers is minimized and the ultimate shear modulus is increased. Similar observations were observed by Vivet et al. in the case of load transfer in carbon fiber reinforced composites [62].

The elongation at break showed their value gradually increase with increasing MWCNT loading (from 1 to 3 wt%), follows the same trend as that of shear strength. An increasing trend of elongation of break may be attributed to the increase in cross-link density with an addition of MWC-NTs. However, as the amount of the MWCNT is increased beyond percolation threshold (i.e. at 5 wt%), the adhesive has become more brittle and this resulted in the reduction of elongation at break. Additionally by increasing the amount of MWCNTs, the partially separated micro spaces between the MWCNTs and the polymer matrix obstructs stress propagation from the polymer matrix to the filler. This induces decreased strength and increased brittleness that would make the elongation of the whole adhesive somewhat difficult when subjected to tensile loading [63]. It can be observed that, in case of epoxy/MWCNT/VGCF adhesive at higher strain the orientation of the polymer chains into the agglomerates may reach the limitation of finite chain extensibility, so that the deformation everywhere in the adhesive, including the crack tip is bounded. Thus higher stress at a given elongation is obtained [64].

From Fig. 10 a typical stress–strain response of the pure epoxy and epoxy/MWCNT adhesive with the filler content of 1, 2, 3, 5 and 3 wt% of MWCNT with 3 wt% of VGCF is illustrated. Linear stress–strain relation was observed in all the epoxy adhesives until it breaks, before the stress level reaching the maximum value. All the samples imparted brittle failure as indicated by a sudden drop in the peak stress.

Based on the major failure modes in epoxy adhesives, a correlation between the adhesive failure and stress–strain response has been established. In addition, different failure modes were observed for epoxy adhesives as shown in Fig. 11. The mode of failure for epoxy was found to be adhesive [2]. This depicts brittle fracture mode of epoxy and this consideration shows the good agreement between low shear strength and elongation at break values. However in case of epoxy adhesive reinforced with 2 wt% of MWCNTs, the failure mode changing from adhesive to mixed adhesive/cohesive or partly cohesive mode, determine the bonding effectiveness of adhesive. Similar observation was also observed by Guden et al. [65] in the case of epoxy/CNT adhesive. Another interesting finding was that the failure mode shifted from adhesive (along the bonding interface between substrate and adhesive) for the pure epoxy to purely cohesive for the epoxy incorporated with 3 wt% of MWCNT and 3 wt% of MWCNT with 3 wt% of VGCF content. At higher concentration of MWCNTs, interfacial shear strength between

Fig. 11 Failure mode for epoxy (**a**), epoxy/2 wt% MWCNT (**b**), epoxy/3 wt% MWCNT (**c**) and epoxy/3 wt% MWCNT/3 wt% VGCF (**d**) adhesive system

Adhesive failure

Partially cohesive failure

Cohesive failure
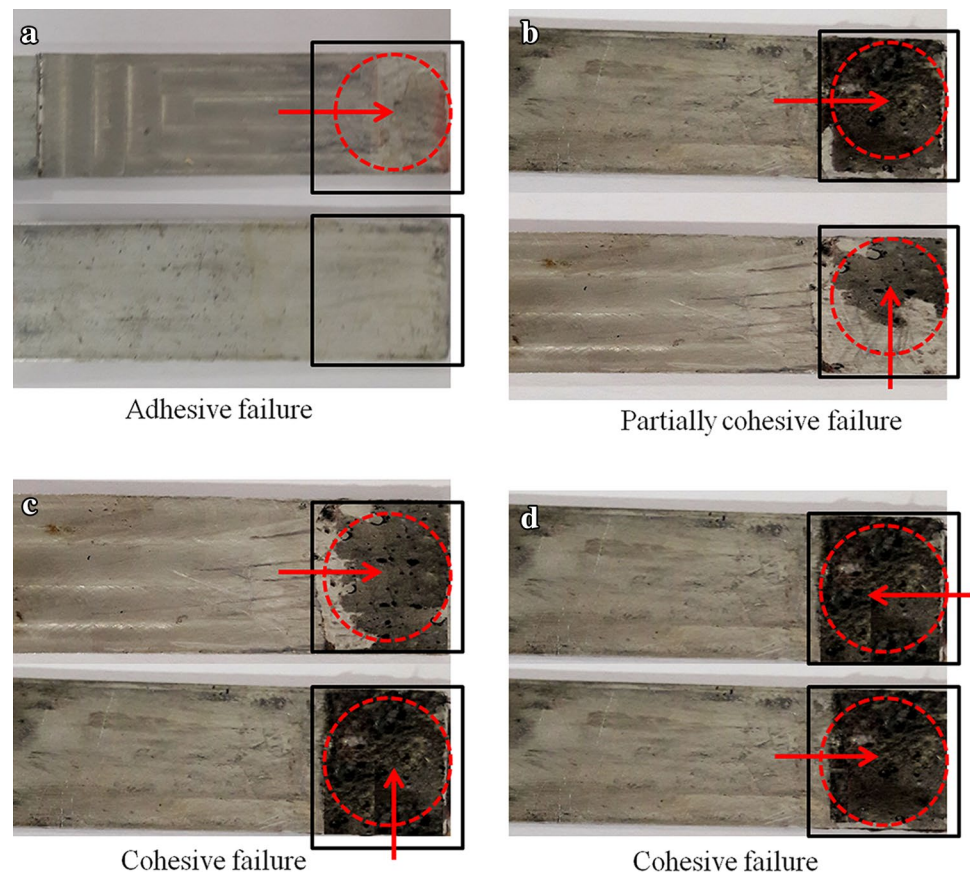
Cohesive failure

the adhesive and the adherent improved and prevented crack intiation and propagation along the interfaces under stress by changing the failure mode to fully cohesive. Hence a correlation between the adhesive failure and stress–strain response of the adhesive is established and confirmed by the higher strain percentage at break for epoxy/MWCNT/VGCF adhesive system [2].

4.4 Scanning electron microscopy (SEM) analysis of epoxy adhesive system

Figure 12 shows the fractured surfaces of the epoxy, epoxy/3% MWCNT and epoxy/3% MWCNT/3% VGCF adhesive system. There is an apparent difference in the fracture behaviour of all epoxy adhesive system. SEM micrograph as shown in the Fig. 12a of the pure epoxy exhibits relatively smooth and featureless fractured surface. Whereas, prominent roughness was observed in the case of reinforced epoxy adhesive systems.

The SEM micrographs of the epoxy incorporated with 3 wt% of MWCNT as shown in Fig. 12b, c has been done to investigate the microscopic changes associated with the inclusion of MWCNTs in the polymer matrix. SEM micrographs showed in Fig. 12b exhibits a typical brittle fracture pattern in between the MWCNTs. This indicates the formation of a strong interfacial adhesion between MWCNTs and polymer matrix. Also the fractured adhesive surface is much rough and their crack becomes more random. This is probably due to resistance to crack propagation through blocking the growing voids by MWCNTs. This type of crack propagation is irregular that is evident from waviness of a nearly flat surface in the SEM micrographs of epoxy/MWCNT adhesives. Furthermore when the tensile loading increases, the crack length will increase in the weak area of the MWCNTs network. SEM micrograph as shown in Fig. 12c reveals MWCNT fractured and shrinkage along the length. MWCNTs gradually shrink with increasing tensile loading. This indicates that MWCNTs will burst out once stress reaches their maximum value [66].

In the case of epoxy/3% MWCNT/3% VGCF adhesive system as shown in Fig. 12d, e the filler particles are appeared to be completely covered by the polymer matrix, which indicates good interfacial adhesion between the filler particles and polymer matrix. Figure 12d shows that the crack started from the interface, and then VGCF suffered from the external force along with VGCFs were pulled out of adhesives leaving the smooth polymer matrix. This revealed great effect of VGCF on the interfacial bonding as well as load effectively gets transferred from the matrix to the filler particles. Based on the morphological observations, one can say that why the mechanical properties are high in case of epoxy/MWCNT/VGCF adhesive system.

4.5 Thermo-gravimetric analysis (TGA) of epoxy adhesive system

TGA was carried out to analyse the thermal degradation behaviour of different epoxy adhesive formulations. Figure 13a and b shows the TG-DTG thermograms of pure epoxy, epoxy/3% MWCNT and epoxy/3% MWCNT/3% VGCF adhesive system.

From Fig. 13a it can be seen that epoxy incorporated with 3 wt% of MWCNT and VGCF showed higher thermal stability as compared to epoxy/3% MWCNT adhesive system. This improvement in thermal stability is mainly attributed to the homogeneous dispersion and formation of strong interface between filler particles and polymer matrix. Strong interfacial adhesion resulted in the reduction of the mobility of the polymer molecular chains, which lead to a significant increase in thermal stability of epoxy/MWCNT/ VGCF adhesive system [32].

A two-step degradation process was observed for all three epoxy adhesive formulations. In the case of epoxy, initial decomposition is observed at 313–380 °C followed by final decomposition in the range of 450–610 °C. Furthermore, with the addition of 3 wt% of MWCNT within epoxy elucidates significant increase in thermal stability with the appearance of initial decomposition in the range of 310–450 °C. This behaviour indicates pyrolysis of the epoxy resin network and dehydration of the hydroxyl groups [67]. For epoxy/3% MWCNT adhesive, the final decomposition was observed at 480–700 °C, elucidates complete decomposition of the unreacted long chain fragments of epoxy resin. Similar finding was reported by Park et al. [68].

For epoxy incorporated with 3 wt% of MWCNT and VGCF, the first-stage decomposition starts around 298–470 °C, which is attributed to the evaporation and decay of the unreacted small species such as carbonyl, methoxy and ester. The second-stage decomposition around 440 °C is possibly due to the degradation of the higher molecular weight three dimensional network structure of epoxy formed after curing. The second stage decomposition above 500 °C is related to the degradation of small fragments with more char residue. Although initial degradation occurs at a higher temperature, the first sharp degradation of the epoxy incorporated with 3 wt% of MWCNT begins at a higher temperature in comparison with epoxy/MWCNT/VGCF adhesive system.

From DTG thermo gram as shown in Fig. 13b it is found that all three epoxy adhesive formulations shows two peaks corresponding to the maximum rate or degradation, T_{p1} and T_{p2}. For pure epoxy the maximum rate of degradation corresponding to T_{p1} and T_{p2} occurred at 380 and 560 °C. Whereas, epoxy/3% MWCNT shows two peaks corresponding to the maximum rate of degradation, T_{p1} and T_{p2} at 352 and 552 °C, respectively. Similarly, epoxy incorporated with
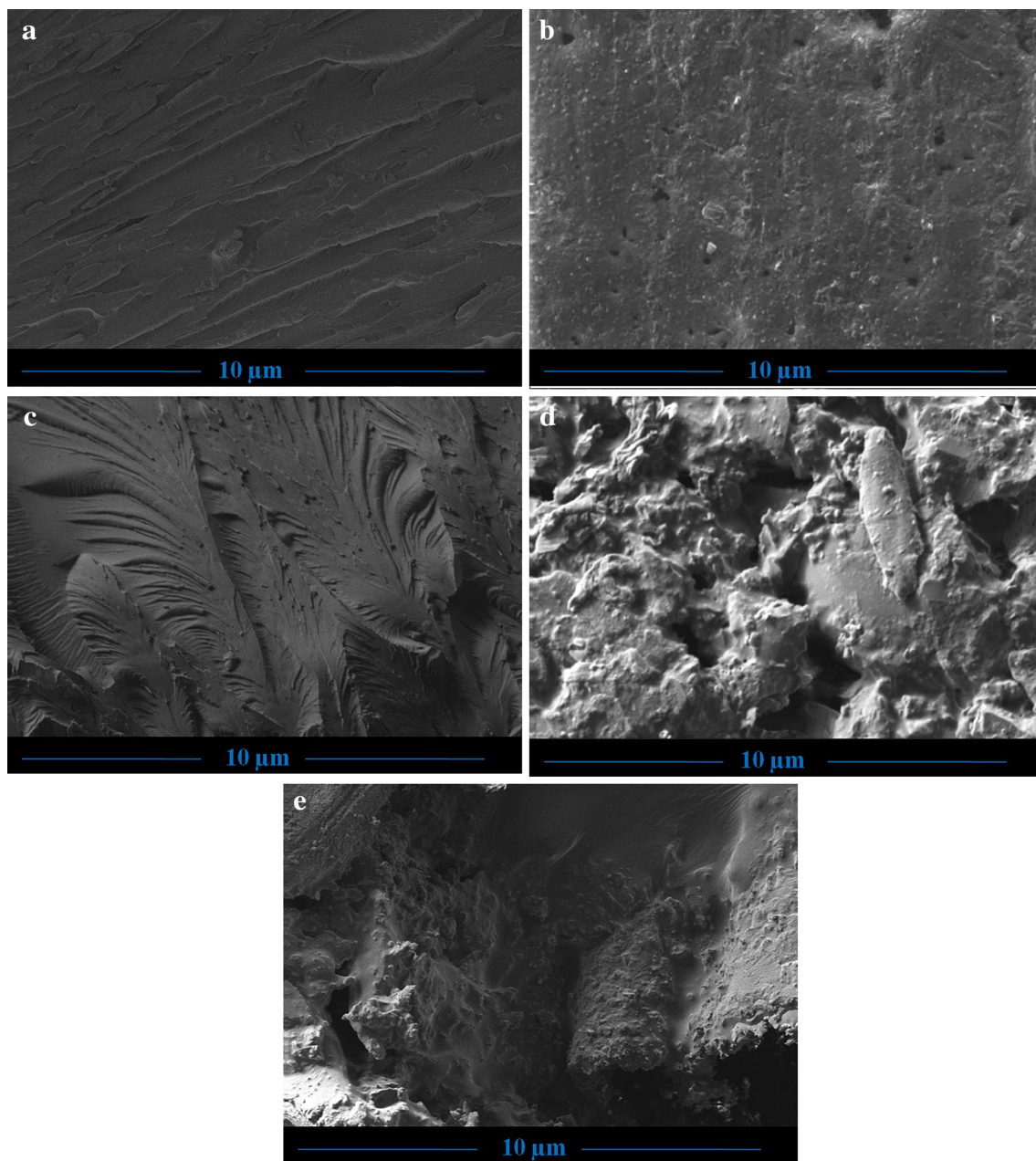
Fig. 12 SEM images of the fractured surfaces of epoxy (**a**), epoxy/3% MWCNT (**b, c**) and epoxy/3% MWCNT/3% VGCF (**d, e**) adhesive system

3 wt% of MWCNT and VGCF exhibits two peaks at T_{p1} of 368 °C and T_{p2} value of 572 °C. It is noteworthy that for epoxy/3 wt% MWCNT adhesive system the maximum rate of degradation occurred at a considerably lower temperature than the epoxy incorporated with 3 wt% of MWCNT and VGCF. The considerably lower rate of degradation and shift in the peak towards a higher temperature reveals the greater thermal stability of epoxy/MWCNT/VGCF adhesive system. This behaviour can be attributed to the restricted mobility of

filler particles inside the cross-linked epoxy adhesive system [67]. Similar finding were also observed by Borugadda [69] and Hardis et al. [70].

4.6 Dynamic mechanical analysis (DMA) of epoxy adhesive system

Figure 14 shows the DMA curves of storage modulus (E') and loss modulus (E'') as a function of temperature for pure
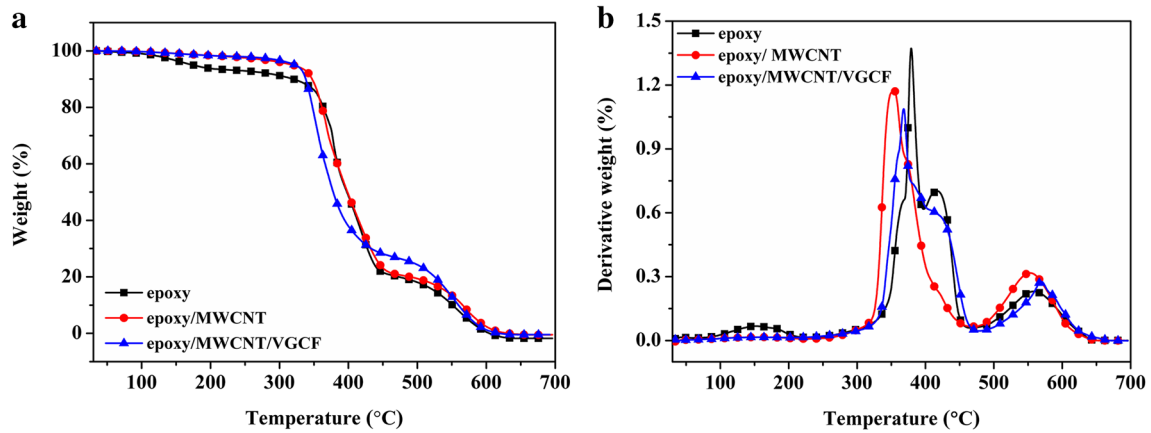
Fig. 13 TGA (**a**) and DTG (**b**) thermogram of epoxy, epoxy/3% MWCNT and epoxy/3% MWCNT/3% VGCF adhesive system
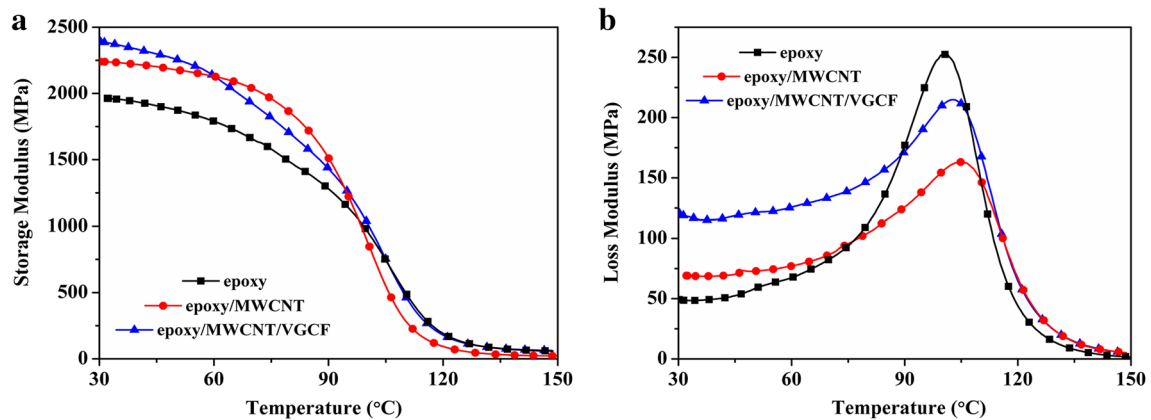

Fig. 14 Variation of storage modulus (**a**) and loss modulus (**b**) as a function of temperature for all three epoxy adhesive system

epoxy, epoxy/3% MWCNT and epoxy/3% MWCNT/3% VGCF adhesive system and important findings were summarized in Table 4.

From Table 4, it is observed that the epoxy incorporated with 3 wt% of MWCNT and VGCF exhibits a higher storage modulus than epoxy/3% MWCNT adhesive. Epoxy incorporated with MWCNT and VGCF showed storage modulus value of 2400 MPa, which is approximately 7% and 22.4% increase in storage modulus at 30 °C, as compared to epoxy/3% MWCNT and pure epoxy, respectively. This increase in storage modulus is most likely related to the strong interfacial adhesion between fillers and polymer matrix in epoxy/MWCNT/VGCF framework. Strong interfacial adhesion restricts the molecular movement of polymeric chains, consequently modulus increases [71–73]. Whereas the decreased value of storage modulus for epoxy incorporated with 3 wt% of MWCNT, is attributed to the hindrance in the formation of three dimensional crosslinked network structure of epoxy, due to the presence of MWCNTs [72].

Table 4 DMA results obtained for pure epoxy, epoxy/3% MWCNT and epoxy/3% MWCNT/3% VGCF adhesives

Sample type	Storage modulus (MPa)	Loss modulus (MPa)	Glass transition temperature (T_g, °C)
Epoxy	1960	48	118
Epoxy/3 wt% MWCNT	2245	69	115
Epoxy/3 wt% MWCNT/3 wt% VGCF	2400	120	112

Additionally, epoxy incorporated with 3 wt% of MWCNT and VGCF yielded 73.9% and 150% increase in loss modulus at 30 °C, respectively, over epoxy/3% MWCNT and pure epoxy. It is attributed due to the presence of higher modulus VGCF fibers, that minimizes the flexibility of the polymeric chains by limiting their segmental immobility [74]. Moreover, due to the addition of MWCNT and VGCF within epoxy, peak height of loss modulus curve is higher

than that of epoxy/MWCNT adhesive system. This suggests that hybrid effect of MWCNT and VGCF dissipates some energy due to the visco-elastic deformation at the filler-matrix interface.

The loss factor, tan δ as a function of temperature for all three epoxy adhesive systems was measured using DMA and shown in Fig. 15. The peak position temperature of tan δ curve was used to determine the glass transition temperature (T_g) of the epoxy adhesive system and results have been summarized in Table 4. It is clear that the T_g decreases with the inclusion of MWCNT and VGCF within pure epoxy. This indicated that tan δ can be related to interfacial properties and is a true indicator of molecular motion. The decreased T_g can be associated with the restricted movement of the polymeric chain due to the addition of stiffer VGCF fibers. Also, tan δ peak height increases for MWCNT and VGCF infused epoxy. This mechanism can be correlated with the relaxation process that brings about such restraining within the epoxy adhesive owing to the increase in the number of chain segments and more free space upon VGCF incorporation [74].

5 Conclusions

The present study deals with enhancing various properties of pure epoxy by exerting an external electric field for the alignment of MWCNTs. Both aligned MWCNT and VGCF showed a remarkable effect on various properties of pure epoxy adhesive system. The aforementioned findings were concluded from the test results:

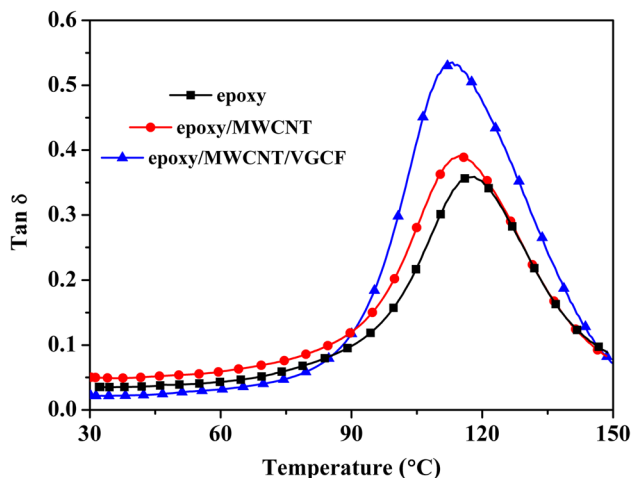(1) SEM and AFM micrographs revealed higher degree of alignment and dispersion of fillers when embed-

Fig. 15 Variation of tan δ as a function of temperature for all three epoxy adhesive system

ded in epoxy resin, proving an alignment as a tool for improved dispersion and avoid aggregation of fillers.

(2) Thermal conductivity was also improved due to aligned interconnected network of fillers within cured epoxy adhesive system. Thermal conductivity of pure epoxy showed an improvement of 225% for 3 wt% of aligned MWCNT/epoxy, whereas, a remarkable 370% increase in T_c was observed for the combined effect of 3 wt% of aligned MWCNT with VGCF filled epoxy adhesive system. The T_c of unaligned MWCNT filled epoxy adhesive system was also measured and test result indicated the strengthening effect of aligned MWCNTs on T_c of epoxy adhesives.

(3) Pure epoxy showed shear strength value of 4 MPa, which increased upto 5.9 MPa (approx. 47.5% increases in strength) with an addition of 3 wt% of MWCNT in polymer matrix. The shear strength again increases and achieved an optimum value of 8.5 MPa with an addition of 3 wt% of MWCNT with 3 wt% of VGCF, confirming the effectiveness of filler particles on mechanical properties of pure epoxy. This increase in strength can be attributed to the uniform dispersion and mechanical interlocking mechanism by increasing the spefic contact area between the filler particles and polymer matrix.

(4) The failure mode of different epoxy adhesive systems was also investigated and a correlation of data was established between failure mode and stress–strain response of epoxy adhesives. It was found that pure epoxy breaks in adhesive mode. Moreover, when the failure mode shifted from adhesive to cohesive higher adhesive strength was achieved. This is confirmed by the higher elongation of break of epoxy adhesive system.

(5) The DMA thermogram showed a higher value of storage and loss modulus for epoxy incorporated with 3 wt% of MWCNT with 3 wt% of VGCF. Whereas, an opposite trend in glass transition was observed for epoxy adhesive systems. The decreased in glass transition can be associated with the addition of VGCF fibers, which causes restriction of chain motion in polymer networks.

(6) TGA indicated higher thermal stability of epoxy adhesive filled with 3 wt% of MWCNT with VGCF. This increase in thermal stability is mainly attributed to the formation of strong interface due to homogeneous dispersion of filler particles in polymer matrix.

References

1. A.K. Singh, B.P. Panda, S. Mohanty, S.K. Nayak, M.K. Gupta, Polym. Adv. Technol. (2017). doi:10.1002/pat.4072
2. A.K. Singh, B.P. Panda, S. Mohanty, S.K. Nayak, M.K. Gupta, J. Mater. Sci. **28**, 8908 (2017). doi:10.1007/s10854-017-6621-3
3. T. Villmow, S. Pegel, A. John, R. Rentenberger, P. Pötschke, Mater. Today **14**, 340 (2011)
4. Y. Li, K.S. Moon, C.P. Wong, *Nano-Conductive Adhesives for Nano-Electronics Interconnection. In Nano-Bio-Electronic, Photonic and MEMS Packaging*. (Springer, New York, 2010)
5. A.Paipetis,V Kostopoulos, *Carbon Nanotube Enhanced Aerospace Composite Materials: A New Generation of Multifunctional Hybrid Structural Composites*. (Springer, Dordrecht, 2012)
6. J.F. Caers, X.J. Zhao, E.H. Wong, C.K. Ong, Z.X. Wu, R. Ranjoo, in Proceedings electronic components and technology conference, vol 1176, (2016)
7. T.F. Zhang, Z.P. Li, J.Z. Wang, W.Y. Kong, G.A. Wu, Y.Z. Zheng, Y.W. Zhao, E.X. Yao, N.X. Zhuang, L.B. Luo, Sci. Rep. **6**, 38569 (2016)
8. K. Balasubramanian, M. Burghard, Anal. Bioanal. Chem. **35**, 452 (2006)
9. P. Gupta, M. Rajput, N. Singla, V. Kumar, D. Lahiri, Polymer **89**, 119 (2016)
10. O. Osazuwa, M. Kontopoulou, P. Xiang, Z. Ye, A. Docoslis, Procedia Eng. **42**, 1414 (2012)
11. D. Domingues, E. Logakis, A.A. Skordos, Carbon **50**, 2493 (2012)
12. M. Monti, M. Natali, L. Torre, J.M. Kenny, Carbon **50**, 2453 (2012)
13. I.C. Finegan, G.G. Tibbetts, J. Mater. Res. **16**, 1668 (2001)
14. G.G. Tibbetts, Carbon **27**, 745 (1989)
15. V.Z. Mordkovich, Theor. Found. Chem. Eng. **37**, 429 (2003)
16. J.E. Jang, S.N. Cha, Y. Choi, T.P. Butler, D.J. Kang, D.G. Hasko, J.E. Jung, Y.W. Jin, J.M. Kim, G.A. Amaratunga, Appl. Phys. Lett. **93**, 113105 (2008)
17. H.E. Troiani, M.M. Yoshida, G.A. Camacho-Bragado, M.A. Marques, A. Rubio, J.A. Ascencio, M. Jose-Yacaman, Nano Lett. **3**, 151 (2003)
18. L.B. Kish, P.M. Ajayan, Appl. Phys. Lett. **93106**, 2004 (2008)
19. J.T. Tsai, H.C. Ko, Appl. Phys. Lett. **88**, 13104 (2006)
20. Y.J. Jung, S. Kar, S. Talapatra, C. Soldano, G. Viswanathan, X. Li, Z. Yao, F.S. Ou, A. Avadhanula, R. Vajtai, S. Curran, Nano Lett. **6**, 413 (2006)
21. L. Zhu, Y. Sun, D.W. Hess, C. Wong, Nano Lett. **6**, 243 (2006)
22. K. Prabakaran, A.K. Palai, S. Mohanty, S.K. Nayak, RSC Adv. **5**, 66563 (2015)
23. H. Sun, X. You, Y. Jiang, G. Guan, X. Fang, J. Deng, P. Chen, Y. Luo, H. Peng, Angew. Chem. Int. Ed. **53**, 9526 (2014)
24. Z. Cai, L. Li, J. Ren, L. Qiu, H. Lin, H. Peng, J. Mater. Chem. A **1**, 258 (2013)
25. Z. Yang, L. Li, Y. Luo, R. He, L. Qiu, H. Lin, H. Peng, J. Mater. Chem. A **1**, 954 (2013)
26. S. Park, M. Vosguerichian, Z. Bao, Nanoscale **5**, 1727 (2013)
27. M. Lee, J. Im, B.Y. Lee, S. Myung, J. Kang, L. Huang, Y.K. Kwon, S. Hong, Nat. Nanotechnol. **1**, 66 (2006)
28. M. Lee, M. Noah, J. Park, M.J. Seong, Y.K. Kwon, S. Hong, Small **5**, 1642 (2009)
29. M.A. Al-Khedher, C. Pezeshki, J.L. McHale, F.J. Knorr, Nanotechnology **18**, 355703 (2007)
30. A.M. Marconnet, N. Yamamoto, M.A. Panzer, B.L. Wardle, K.E. Goodson, ACS Nano **5**, 4818 (2011)
31. S.U. Khan, J.R. Pothnis, J.K. Kim, Compos. Part A **49**, 26 (2013)
32. S.B. Jagtap, D. Ratna, Expr. Polym. Lett. **7**, 329 (2013)
33. A.J. Kinloch, MRS Bull. **28**, 445 (2003)
34. D.S. Kim, C. Baek, H.J. Ma, D.K. Kim, Ceram. Int. **42**, 7141 (2015)
35. F. Ahmadpoor, S.M. Zebarjad, K. Janghorban, Mater. Chem. Phys. **139**, 113 (2013)
36. E.S. Choi, J.S. Brooks, D.L. Eaton, M.S. Al-Haik, M.Y. Hussaini, H. Garmestani, D. Li, K. Dahmen, J. Appl. Phys. **94**, 6034 (2003)
37. S.Y. Kwon, I.M. Kwon, Y.G. Kim, S. Lee, Y.S. Seo, Carbon **55**, 285 (2013)
38. W. Sun, H. Tomita, S. Hasegawa, Y. Kitamura, M. Nakano, J. Suehiro, J. Phys. D **44**, 445303 (2011)
39. Z. Ren, Y. Lan, Y. Wang, *Aligned Carbon Nanotubes Physics, Concepts, Fabrication and Devices*, 1st edn. (Springer, Berlin, 2013)
40. M.G. Zaidi, S.K. Joshi, M. Kumar, D. Sharma, A. Kumar, S. Alam, P.L. Sah, Carbon Lett. **14**, 218 (2013)
41. A.E. Aliev, M.H. Lima, E.M. Silverman, R.H. Baughman, Nanotechnology **21**, 35709 (2010)
42. M.H. Al-Saleh, U. Sundararaj, Carbon **47**, 2 (2009)
43. P. Gonnet, Z. Liang, E.S. Choi, R.S. Kadambala, C. Zhang, J.S. Brooks, B. Wang, L. Kramer, Curr. Appl. Phys. **6**, 119 (2006)
44. J.E. Fischer, W. Zhou, J. Vavro, M.C. Llaguno, C. Guthy, R. Haggenmueller, M.J. Casavant, D.E. Walters, R.E. Smalley, J. Appl. Phys. **93**, 2157 (2003)
45. Y. Zhang, A. Chang, J. Cao, Q. Wang, W. Kim, Y. Li, N. Morris, E. Yenilmez, J. Kong, H. Dai, Appl. Phys. Lett. **79**, 3155 (2001)
46. K. Zhang, M.M.F. Yuen, J.H. Gao, B. Xu, CIRP Ann. Manuf. Technol. **56**, 245 (2007)
47. C.P. Wong, K.S. Moon, Y. Li, *Nano-Bio-Electronic, Photonic and MEMS Packaging*. (Springer, New York, 2010).)
48. Y. Chen, J. Ting, Carbon **40**, 359 (2002)
49. B. Li, S. Dong, X. Wu, C. Wang, X. Wang, J. Fang, Compos. Sci. Technol. (2017). doi:10.1016/j.compscitech.2017.05.006
50. S. Ghose, K.A. Watson, D.C. Working, J.W. Connell, J.G. Smith Jr., Y.P. Sun, Compos. Sci. Technol. **68**, 1843 (2008)
51. H. Huang, C.H. Liu, Y. Wu, S.H. Fan, Adv. Mater. **17**, 1652 (2005)
52. Q. Liao, Z. Liu, W. Liu, C. Deng, N. Yang, Sci. Rep. **5**, 16543 (2015)
53. S.T. Huxtable, D.G. Cahill, S. Shenogin, L. Xue, R. Ozisik, P. Barone, M. Usrey, M.S. Strano, G. Siddons, M. Shim, P. Keblinski, Nat. Mater. **2**, 731 (2003)
54. N. Shenogina, S. Shenogin, L. Xue, P. Keblinski, Appl. Phys. Lett. **87**, 133106 (2005)
55. G. Lin, B.H. Xie, J. Hu, X. Huang, G.J. Zhang, J. Nanomater. **16**, 260 (2015)
56. K.K. Mahato, D.K. Rathore, R.K. Prusty, K. Dutta, B.C. Ray, IOP Conf. Ser. **178**, 12006 (2017)
57. M.B. Salam, M.V. Hosur, S. Zainuddin, S. Jeelani, Open J. Compos. Mater. **3**, 1 (2013)
58. G.V. Ramana, B. Padya, R.N. Kumar, K.V. Prabhakar, P.K. Jain, Indian J. Eng. Mat. Sci. **17**, 331 (2010)
59. V. Causin, C. Marega, A. Marigo, G. Ferrara, A. Ferraro, Eur. Polym. J. **42**, 3153 (2006)
60. M. Hossain, M. Chowdhury, M. Salam, N. Jahan, J. Malone, M. Hosur, S. Jeelani, N. Bolden, J. Compos. Mater. **49**, 2251 (2014)
61. X. Shen, J. Jia, C. Chen, Y. Li, J.K. Kim, J. Mater. Sci. **49**, 3225 (2014)
62. A. Vivet, W. Leclerc, B.B. Doudou, J. Chen, C. Poilâne, Fibers **3**, 134 (2015)
63. M. Sudheer, R. Prabhu, K. Raju, T. Bhat, Adv. Mater. Sci. Eng. **2014**, 1 (2014). doi:10.1155/2014/970468
64. J. Saji, S.P. Mahapatra, J. Basic Appl. Eng. Res. **1**, 33 (2014)
65. M.R. Guden, S.G. Prolongo, T. Gomez-del Rio, A. Urena, Int. J. Adhes. Adhes. **31**, 695 (2011)
66. V.K. Srivastava, S. Singh, Int. J. Compos. Mater. **2**, 1 (2012)
67. S.K. Sahoo, S. Mohanty, S.K. Nayak, RSC Adv. **5**, 13674 (2015)

68. S.J. Park, F.L. Jin, C. Lee, Mater. Sci. Eng. A **402**, 335 (2005)
69. V.B. Borugadda, V.V. Goud, Thermochim. Acta **577**, 33 (2014)
70. R. Hardis, *Cure Kinetics Characterization and Monitoring of An Epoxy Resin for Thick Composite Structures*. Graduate Theses and Dissertations, Paper 12608. (Iowa State University, US, 2012)
71. M. Dehghan, I. Sbarski, Int. J. Chem. Nucl. Metall. Mater. Eng. **8**, 119 (2014)

72. K. Yu, M. Wang, J. Wu, K. Qian, J. Sun, X. Lu, Nanomaterials **6**, 89 (2016)
73. S. Gupta, A. Rahaman, Int. J. Sci. Publ. **5**, 1 (2015)
74. M.I. Reddy, V.S. Reddy, Int. J. Eng. Res. Technol. **3**, 410 (2014)